

# ULRR

## Enzymatic hydrolysis lignin and kraft lignin from birch wood: a source of functional bio#based materials

Item Type	Article
Authors	Ramirez Huerta, Edgar;Muddasar, Muhammad;Collins, Maurice
Citation	Wood Science and Technology
Publisher	Springer
Download date	2026-03-09 15:54:47
Item License	<a href="https://creativecommons.org/licenses/by-nc-sa/4.0/">https://creativecommons.org/licenses/by-nc-sa/4.0/</a>
Link to Item	<a href="https://doi.org/10.34961/researchrepository-ul.25303882">https://doi.org/10.34961/researchrepository-ul.25303882</a>



# Enzymatic hydrolysis lignin and kraft lignin from birch wood: a source of functional bio-based materials

Edgar Ramirez Huerta<sup>1</sup> · Muhammad Muddasar<sup>1</sup> · Maurice N. Collins<sup>1,2,3</sup>

Received: 28 September 2023 / Accepted: 8 January 2024  
© The Author(s) 2024

## Abstract

In the pursuit of sustainable biomass utilization, this study investigates the hydrothermal treatment of birchwood and its subsequent impact on enzymatic hydrolysis lignin (EHL). Additionally, birchwood undergoes processing with NaOH (4% w/w) within a Parr reactor to precipitate lignin from the black liquor, resulting in lignin-rich substrates (LRSs) which are then subject to thorough characterization. Notably, EHL produced after hydrothermal pretreatment at 190 °C exhibits the highest lignin content at 67%, while kraft lignin (KL) obtained at 140 °C (pH 1.5) produces 65% lignin content. Among these LRSs, the KL sample produced at 190 °C (pH 4) stands out, displaying a robust aromatic skeletal structure and an abundance of methoxy groups, primarily owing to its high purity. Furthermore, for these LRSs' it is shown that chemical configuration influences their thermal behaviour, allowing the lignin to be tailored for diverse applications, from low melting point materials to carbonaceous materials capable of withstanding temperatures exceeding 700 °C. This comprehensive understanding of the chemical, thermal, and physical attributes of LRSs not only enriches our knowledge of lignin-rich substrates but also paves the way for the development of sustainable bio-based materials, marking a step towards sustainable materials development.

## Introduction

The ever-increasing consumption of natural resources has propelled the urgent need for sustainable alternatives to conventional materials (Muddasar et al. 2022, 2023a). As our planet faces environmental challenges, the demand for

---

✉ Maurice N. Collins  
Maurice.Collins@ul.ie

<sup>1</sup> Stokes Laboratories, School of Engineering, Bernal Institute, University of Limerick, Limerick V94 T9PX, Ireland

<sup>2</sup> AMBER, University of Limerick, Limerick, Ireland

<sup>3</sup> BiOrbic, University of Limerick, Limerick, Ireland

eco-friendly materials continues to grow. Sustainable materials, derived from renewable sources, have the potential to alleviate the strain on the biosphere while addressing the socio-environmental emergencies that stem from resource depletion. Lignocellulose, an abundant and renewable resource found in forests, crops, and food residues, has emerged as a key player in the pursuit of sustainable materials. Among its components, lignin, the most prevalent aromatic polymer on Earth, holds great promise (Beaucamp et al. 2022a, b).

Lignin, a complex polyphenolic compound, primarily consists of monolignols, including p-coumaryl, coniferyl, and sinapyl alcohol, which serve as precursors in the formation of p-hydroxyphenyl (H), guaiacyl (G), and syringyl (S) units. The paper industry alone generates over 70 million tons of residual lignin, challenging its separation from black liquor and hindering its development into high-performance functional applications (Jędrzejczak et al. 2021). Despite forecasts predicting a billion-dollar market for lignin-based products by 2025, lignin often goes to waste or is relegated to low-value applications, hindering its transition into high-performance, functional materials (Rubio et al. 2022; Muddasar et al. 2023b; Muddasar et al. 2024). The technology readiness level remains low, with less than 2% of lignin being employed for concrete additives, stabilizing agents, dispersants, or surfactants. To unlock lignin's potential, its valorization in advanced energy and engineering applications is of paramount importance (Collins et al. 2019).

Lignin can be obtained as a solid residue from the chemical pulp industry and biofuel production, both of which utilize lignocellulosic biomass and generate substantial quantities of residual lignin (Sharma et al. 2020). While the chemical pulp industry transforms cellulose into paper, yielding a black liquor rich in lignin, the most common fate for this lignin is precipitation and drying as technical lignin, primarily used as a solid fuel. In contrast, biofuel production involves the conversion of cellulose into bioethanol through pretreatment, hydrolysis, and fermentation. The enzymatic process, intended to remove sugars, often results in lignin carbohydrate complexes, which are frequently discarded as solid fuel to meet the energy demands of fermentation and distillation operations. However, efficient enzymatic degradation of cellulose and hemicellulose fractions can yield cleaner lignin by-products, closer in composition to native lignin, and suitable for high-value applications (Lu et al. 2020; Sharma et al. 2020).

Clean lignin, with minimal contaminants, opens doors to the development of high-value products, including biomedical substrates, carbon fibre precursors, bio-adhesives, UV lignin blockers, energy storage additives, and smart materials such as thermogelling copolymers for tissue engineering (Albadarin et al. 2017; Beaucamp et al. 2019, 2024; Collins et al. 2019; Culebras et al. 2018a; Dalton et al. 2019). The valorization of lignin has the potential to transform bioethanol and pulp industries into biorefineries, capable of producing bio-based materials that replace conventional fossil-based consumables and engineered materials. Thus, a comprehensive study is necessary to optimize the delignification process parameters for clean lignin production, which will provide valuable insight into the challenges and opportunities pertaining to lignin valorization, paving the way for a sustainable and resource-efficient future.

This study seeks to comprehensively understand the diverse properties of lignin, which can vary due to factors such as biomass source and processing methods. It involves four main objectives: (1) producing and characterizing lignin rich substrates (LRSs) through enzymatic hydrolysis and kraft process black liquor acidification, (2) assessing the impact of hydrothermal pretreatment on cellulase performance for high-purity lignin production, (3) evaluating different kraft lignins characteristics produced under varying conditions, and (4) comparing Enzymatic Hydrolysis Lignins (EHLs) and Kraft Lignins (KLs) for their suitability in bio-based materials. The results of this research provided valuable principles, data and instructions covering multiple features that support the valorization and development of lignin-based materials. This research employs advanced techniques to examine lignin's composition, elemental configuration, chemical structure, thermal behaviour, morphology, and porosity. It also introduces an innovative method for producing chemically pure lignin and addresses the crucial question of lignin purity requirements. This knowledge will enable scientists and engineers to develop new materials based on lignin, such as bioplastics, composites, and coatings. Additionally, the research provides insights into the potential applications of lignin in the energy sector.

## Experimental section

### Materials

The milled birch wood employed in this study (MBW) was supplied by Sappi Europe SA and Vertoro (Sittard-Geleen, Nederland). Sodium azide, sodium hydroxide, and sulphuric acid were purchased from Sigma-Aldrich, Ireland. The enzyme used was “Cellulase, enzyme blend” supplied by Sigma, UK.

### Hydrothermal pretreatment of birch wood

The as received birch wood was air-dried until constant weight, milled to homogeneous particle size (~ 0.5 mm) and stored in a sample plastic box at room temperature until further use. The experimental scheme followed in this study is illustrated in Fig. 1. Hydrothermal pretreatment of the MBW was carried out at Celignis Limited using an Accelerated Solvent Extractor, Dionex ASE-200 (Thermo Scientific, USA). First, 6.25 g of MBW were loaded into a 33 ml stainless steel extraction cell fitted with two polyester filters. Next, the extraction cell was closed from the head and sealed inside a compression oven. Next, the pretreatment liquid was displaced using a line connected to a needle mechanism fitted in a collection vial containing 1 ml of aqueous sodium azide (0.02% w/w). Water was used as the pretreatment solvent and pumped into the cell until reaching 1500 psi, indicating complete filling of the 33 ml sample cell. The cell was then heated until pretreatment temperature (170, 190, 200 °C) for 10–14 min, respectively. The pretreatment lasts for 1 h, also known as the auto-hydrolysis phase, where the hemicellulose and most extractives get dissolved. A vent valve regulates the pressure during pretreatment to maintain it

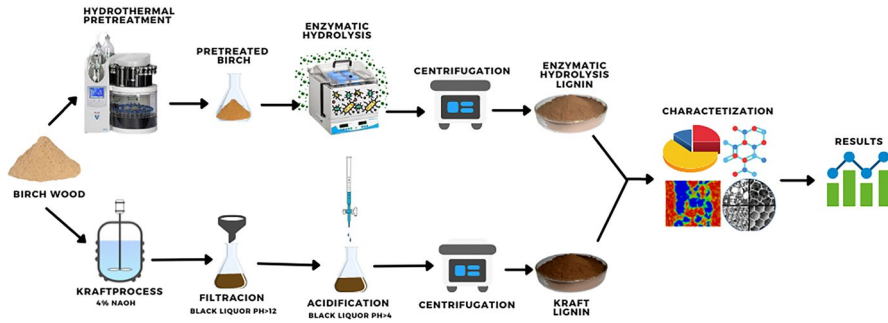


**Fig. 1** The experimental scheme to produce enzymatic hydrolysis lignin and kraft lignin

at 1500 psi ( $\pm 200$ ). Once the pretreatment finished (1 h), the compression oven was switched off with a subsequent cool-down of the compression oven to 85 °C using an air gun. The pretreatment liquor was then rinsed in a collection vial with nitrogen as a purge gas for 10 min. After complete purge of the cell, the collection vial was changed to a new vial with 1 ml of Sodium Azide 0.02% (w/w) to collect the 33 ml washings. After washing, the residual pressure was vented out, and the cell was unloaded from the oven. The hydrothermally pretreated birch wood (labelled HTBW) was meticulously removed from the cell, placed into a sample tray, and air-dried overnight at 50 °C. The HTBW was then stored in a sample plastic box at room temperature until further use.

### Enzymatic hydrolysis of hydrothermally pretreated birch wood

Enzymatic hydrolysis of the HTBW was carried out using Erlenmeyer flasks placed on an orbital agitation bath (Julabo, Germany) set up at 200 rpm with 6% of dried solids loading. The HTBW was suspended in a 0.05 M citric-acid sodium citrate buffer. The enzyme-to-solid ratio was fixed at 30, 55, and 100 mg/g glucan. The solution was incubated for 72 h at 50 °C. After 72 h, the enzymatic hydrolysis solid residue, termed EHL was collected by centrifugation and placed into a sample tray for air drying overnight at 50 °C. The EHL was stored in a sample plastic box at room temperature until further use.

### Kraft process of birch wood

The MBW was subject to hydrothermal processing with a solution of sodium hydroxide (4% w/w) using a stainless-steel (316L) Parr reactor, Model YZPR-1000 ml (Yan Zheng Instrument, China) to precipitate the lignin dissolved in the black liquor. Approximately 40 g of sample were placed in a PTFE reaction vessel, mixed with 360 ml of sodium hydroxide solution, and stirred by hand until a homogeneous solution was obtained. The reaction vessel was subsequently placed into a Parr reactor stirring at 50 rpm during the first 20 min of the heating ramp using a double paddle mechanism. The reaction conditions were set for 1 h at 140, 170 and

190 °C. Next, the reactor was switched on, and the heating ramp took one hour to hit the target temperatures. Once the target temperature was achieved, the reaction was kept for one hour with subsequent cooling down to 70 °C. Then the reaction slurry was filtered with a ceramic funnel dressed in a triple layer of polyester fabric with a paper filter between each layer. Finally, the alkali treatment liquid, also known as black liquor, was stored at 4 °C until further use.

### Lignin precipitation from black liquor

The black liquor's initial pH was 12–13, depending on the reaction. The black liquor was acidified with sulphuric acid (3 M) and centrifuged to collect the kraft lignin precipitates. The precipitation procedure was done at room temperature in a 500 ml glass beaker using ca. 250–300 ml of black liquor while continuously agitating by hand with a glass rod. Sulphuric acid (3 M) was added dropwise to a final pH between 4.1 and 4.2. The black liquor turned into a light brown liquor where a precipitate could be observed. The light brown liquor solution at ~pH 4 was then centrifuged at 10,000 rpm for 20 min, and the pH 4 supernatant was collected by pouring it out from the centrifuge tube and stored in a plastic container until further use. When the supernatant was poured out from the centrifuge tube, care was taken to ensure a clean supernatant without suspended solids. The lignin-rich precipitate at pH 4 (LG4) was air-dried overnight at 50 °C, collected and stored until further use. During acidification, the volume of sulphuric acid used was constant and always corresponded to the initial black liquor volume.

The second precipitation step took the pH 4 supernatant through the previously described process. Thus, the sulphuric acid was added dropwise to a final pH between 1.5 and 1.6. Next, the ~pH 1.5 solution was centrifuged at 10,000 rpm for 20 min. After centrifugation, the supernatant was poured out carefully from the centrifuge tube, leaving the tube with a wet precipitate pellet that was further air-dried overnight at 50 °C. The lignin-rich precipitate at pH 1.5 (LG1.5) was collected and stored until further use.

### Material characterization

Lignin and residual carbohydrates in birch wood and LRSs were analysed following the national renewable energy laboratory (NREL) methodology. Elemental analysis (C, H, N, S) was conducted according to European Standard EN 15104:2011 (Sluiter et al. 2008). For thermal characterization, differential scanning calorimetry (DSC) and thermogravimetric analysis (TGA) were utilized to understand structural influences on thermal behaviour and stability. Structural characterization was performed using Fourier transform infrared spectroscopy (FTIR) and nuclear magnetic resonance spectroscopy (NMR). Physical characterization included surface area and pore size distribution (PoSD) analysis, as well as scanning electron microscopy (SEM) for morphological observation. Detailed characterization details can be found in the supporting information section.

## Results and discussion

### Enzymatic hydrolysis process: lignin composition

Hydrothermal pretreatment was conducted on MBW samples prior to enzymatic hydrolysis using pressurized hot water. For hardwoods, the hemicellulose fraction dissolves into the pretreatment liquid via water ions reacting with acetyl groups producing acetic acid (Galbe and Wallberg 2019; Ståhl et al. 2018). As expected higher temperatures increase the dissolution ratio of hemicellulose, however excess heat may cause degradation of cellulose and lignin (Borrega et al. 2011). This pretreatment allows cellulase to digest cellulose more easily due to easier access (Dávila et al. 2019). MBW was hydrothermally pretreated at 170, 190, and 200 °C. The pretreated BW was analysed according to NREL procedure “Determination of Structural Carbohydrates and Lignin in Biomass” (Hayes 2013). Results show that the lignin purity increases from an initial 22.7% for the MBW to 49.3% for the sample pretreated at 200 °C (Fig. 2a) which is mainly attributed to the extraction of hemicellulose which decreased from 23.6 to 0.1%, (Table S1). These results indicate that as the operating temperature increases, acetyl groups present in hemicellulose turn into acetic acid, resulting in the pH of the pretreatment liquid decreasing from 3.5

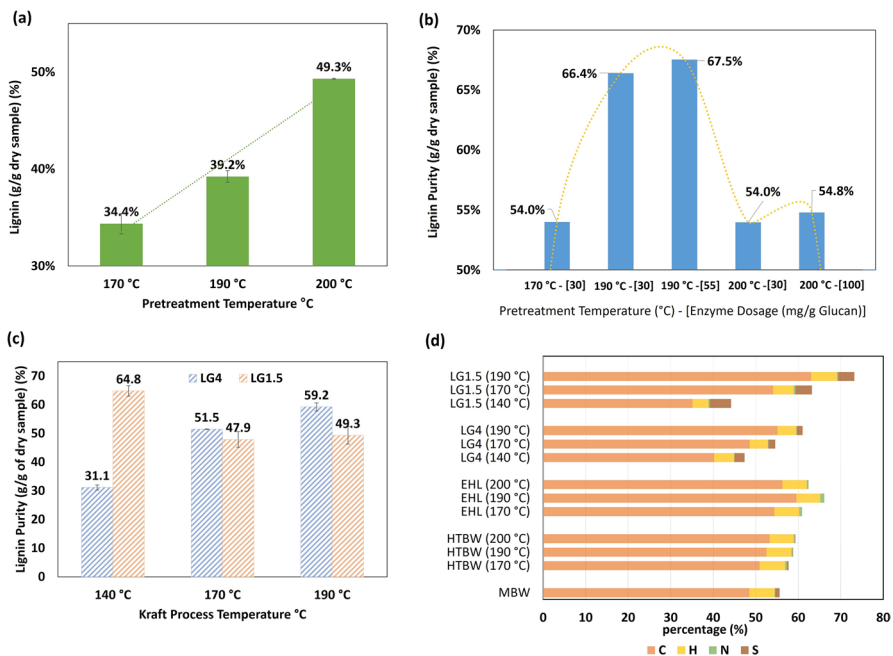


**Fig. 2** Lignin content in **a** hydrothermally treated birch wood produced utilizing accelerated solvent extraction, **b** enzymatic hydrolysis lignin produced using cellulose active enzymes, **c** kraft lignins produced at varying temperature and pH, **d** elemental analysis of untreated milled birch wood, pretreated birch wood and lignin-rich substrates utilizing an Elementar Macro Cube elemental analyser

to 3.2, thereby enhancing dissolution which in turn improves lignin purity. Also, the ash content of the HTBW decreases to minimal levels, which is a positive result as enzymes tend to be affected by elements such as silica within the ash (Hayes 2013). These results are in agreement with previously published data for hydrothermally pretreated birch wood (Borrega et al. 2011; Dávila et al. 2019; Ståhl et al. 2018). However, it should be noted that the importance of pretreatment temperature is evident in these studies as high levels of lignin extraction into pretreatment liquids is reported when the pretreatment temperature is 240 °C indicating that pretreatment temperatures above 200 °C can have a leaching effect of lignin from the pretreated sample itself. Similar results were published for hydrothermally pretreated pine wood showing up to 35% solubilized lignin at 240 °C after only a few minutes of hydrothermal pretreatment.

Enzymatic hydrolysis of pretreated biomass is a common step for producing bioethanol and other bio-based materials (Ewanick et al. 2007; Hu et al. 2006; Nakagame et al. 2011; Trubetskaya et al. 2020). Here, we evaluate the influence of the pretreatment on enzymatic hydrolysis, the enzyme efficiency is correlated to the lignin content in the enzymatic hydrolysis residue, which we denote as enzymatic hydrolysis lignin (EHL). The enzyme dosage effect on the lignin content (purity) of the EHL is also evaluated. Samples were treated at various enzyme-to-solid ratios namely 30, 55, and 100 mg/g glucan, as shown in Fig. 2b. The first experiments were run under an enzyme-to-solid ratio of [30 mg/g glucan]. The results show a beneficial impact on the lignin content (~67%) when the temperature increased from 170 to 190 °C. However, when the pretreatment temperature increased from 190 to 200 °C, the lignin content decreased (54.0%). Thus, the bell curve distribution suggested the existence of an optimal hydrothermal pretreatment temperature corresponding to 190 °C.

Aiming to enhance the lignin content of the samples, the enzyme dosage was increased to [55 mg/g glucan] for the sample treated at 190 °C and to [100 mg/g glucan] for the sample treated at 200 °C. However, the results were equivalent to the previous dosage, with lignin values of 67.5% and 54.8%, recorded, respectively. Table S2 shows the enzyme performance as measured in terms of residual cellulose in the form of glucose. Glucose shows an initial value of 30.1%, decreasing to an optimal value of 24.1% at 190 °C, while 38.9% glucose is recorded at 200 °C. Hence, these results suggest that the enzyme digestion capacity reaches its limit under the current experimental design at 1 h of hydrothermal pretreatment at 190 °C with subsequent enzymatic hydrolysis with an enzyme dosage of 30 mg/g of glucan up to 72 h. While it is known that lignin can act as a physical barrier to enzyme action, steric hindrance prevents the interaction of the enzyme with the accessible cellulose (Mooney et al. 1998). It can also be postulated that enzymes are adsorbed onto lignin instead of cellulose due to hydrophobic, electrostatic, or hydrogen bonding interactions which may explain the detrimental performance of the enzyme on the sample pretreated at 200 °C.

The kraft process is used to treat wood fibres in an alkaline solution composed of sodium hydroxide at temperatures above 140 °C, which leads to the delignification of wood, making lignin available via precipitation. Lignin depolymerization occurs through the cleavage of non-phenolic  $\beta$ -ethers with further entrapment of quinone

methide intermediates. The kraft process substitutes labile C–O bonds in the native lignin by C–C bonds that require higher dissociation energies (Collins et al. 2019; Rinaldi et al. 2016).

MBW was treated with a 4% NaOH aqueous solution for one hour at 140, 170, and 190 °C. After precipitation of the black liquor, a viscous agglomerate of lignin was formed at 140 °C. This is attributed to the xylose content. While darker and more crystalline lignin's were formed at 190 °C, and this is attributed to sugar content (Araújo et al. 2020; Helander et al. 2013). The kraft lignin composition is shown in Table S3.

The effectiveness of the precipitation is assessed by the lignin content in the lignin-rich substrates. For example, LG4 (produced at 140 °C) shows the lowest lignin content, which was expected since the kraft process typically takes place at temperatures of 165–175 °C depending on the delignification targets (see Fig. 2c) (Patt et al. 2000). Samples tended to exhibit high ash content (> 20%) as shown in Table S3, which can be removed by acid/water washings (Chang et al. 1975; Hu et al. 2006; Nakagame et al. 2010, 2011).

### Elemental analysis of LRSs

The composition of the LRSs (EHL, LG4, LG1.5) is evaluated based on their lignin, carbohydrates, and ash content and all samples have alterations in their elemental composition as a result of processing. For example, the EHL sample contains nitrogen associated with enzymatic action on the chemical structure that has absorbed onto lignin instead of acting on the cellulose and this is attributed to a combination of hydrophobic, electrostatic, and hydrogen bonding interactions. While, kraft lignin contains sulphur as a result of acidification in the form of thiol groups added at the  $\beta$ -position of the propane side chain (Hussin 2014; Zhu and Theliander 2015). Moreover, the carbon and hydrogen content of samples provide valuable information related to the polymeric chain degree of modification post-treatment as shown in Fig. 2d. The carbon content of the samples was in the range of 63.0–35%, corresponding to the temperatures at 190 °C and 140 °C. The higher carbon content of the kraft lignin corresponding to the processing temperature of 190 °C can be attributed to labile bonds (C–O, C–H, and O–H) being transformed into cross-linked C–C bonds, which results in a decreased hydrogen content in those samples (Rinaldi et al. 2016). On the other hand, the hydrothermally pretreated birch wood HTBW and EHLs present a carbon content in the range of 40 to ~60%, and these results are as expected for LRSs (Chen et al. 2015; Wądrzyk et al. 2021; Zhao et al. 2014).

### Spectroscopic analysis of LRSs structure

FTIR is utilized to evaluate the presence of residual carbohydrates. The corresponding bands were assigned according to the references in Table S4, and the spectra results are shown in Fig. 3a. The spectral profiles show distinctive lignin-related bands at 1595, 1513, and 1423  $\text{cm}^{-1}$ , representing the aromatic skeleton. Spectra show broad bands at 3460–3390  $\text{cm}^{-1}$  related to the stretching

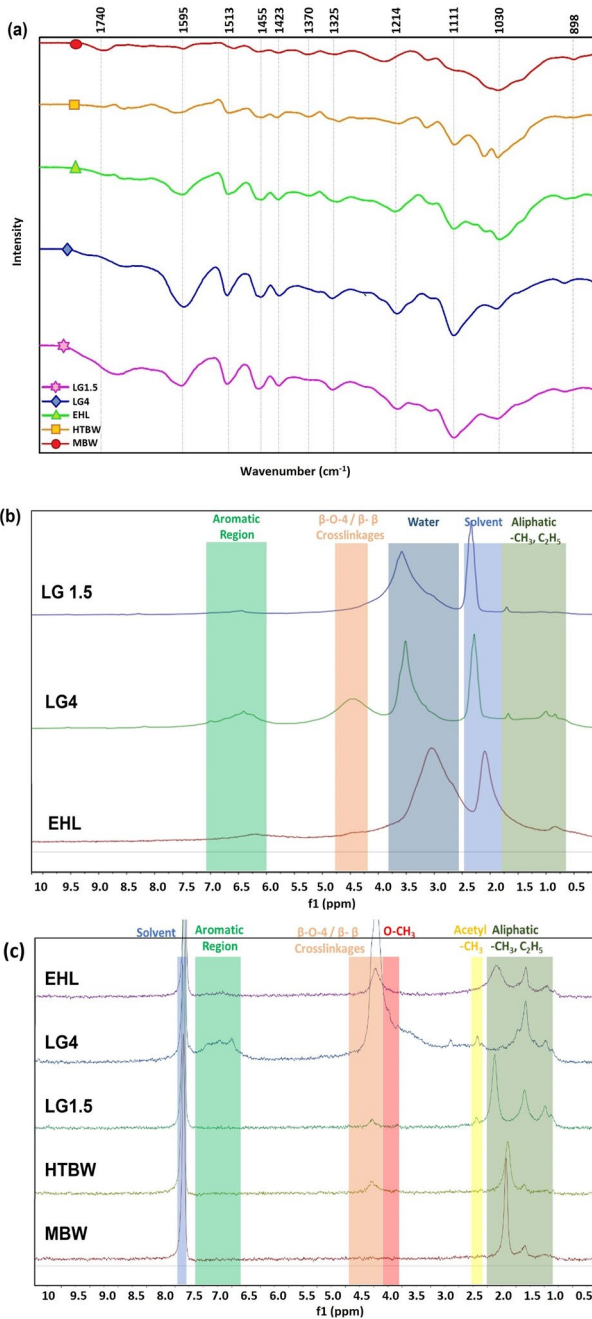


**Fig. 3** a FTIR spectra of lignin-rich substrates produced by enzymatic hydrolysis or kraft process; b <sup>1</sup>H NMR in DMSO for EHL, LG4 and LG1.5; c <sup>1</sup>H NMR for EHL, LG4, LG1.5, HTBW, MBW in chloroform

vibration of hydroxyl groups. The stretching of methyl ( $\text{CH}_3$ ) and methylene ( $-\text{CH}_2-$ ) groups at  $2853$  and  $2960$ – $2933$   $\text{cm}^{-1}$ , respectively, and the vibration at  $1455$   $\text{cm}^{-1}$  correspond to C–H bending in the fingerprint region. The presence of carbonyl C=O group of unconjugated structures at  $1738$ – $1593$   $\text{cm}^{-1}$ . The presence of Syringyl (S) units was observed with vibrations around  $1325$ ,  $1111$ , and  $813$   $\text{cm}^{-1}$ . While the Guaiacyl (G) unit was observed at  $1214$  and  $1030$   $\text{cm}^{-1}$ .

The MBW shows a small band at  $1740$  and  $1030$   $\text{cm}^{-1}$  related to hemicellulose and another minor band at  $898$   $\text{cm}^{-1}$  related to cellulose. Those bands were not present in LRS samples. The HTBW did not exhibit the band at  $1740$   $\text{cm}^{-1}$ , and this confirms the effectiveness of the pretreatment, which is further supported by the residual carbohydrates analysis. Peaks at  $1595$ ,  $1513$ , and  $1423$   $\text{cm}^{-1}$  relate to the aromatic skeletal nature of lignin and are only present in the LRSs. The EHL shows more prominent aromatic skeletal vibrations than the HTBW, confirming the concomitant enzymatic hydrolysis effect for enriching the lignin content of the remaining substrate. With, LG4 and LG1.5 exhibiting the most intense aromatic skeletal vibrations, which is attributed to their higher purity. Among the LRSs, only the EHL shows a small band at  $1370$   $\text{cm}^{-1}$  related to aliphatic C–H stretching in  $\text{CH}_3$  (not in  $\text{OCH}_3$ ) and this highlights that the integrity of the lignin polymer remains after hydrothermal pretreatment and enzymatic hydrolysis as a result of milder conditions (Rinaldi et al. 2016).

The LRSs of this study correspond to guaiacyl (G), and syringyl (S) units, GS 4 lignins, (which have higher  $\beta$ -O-4 content) demonstrated by the band at  $1455$   $\text{cm}^{-1}$  that was essentially more intense than the band at  $1513$   $\text{cm}^{-1}$ . Additionally, the band at  $1111$   $\text{cm}^{-1}$  was dominant, and there was no band at  $1266$   $\text{cm}^{-1}$ . Therefore, inferring from previous studies of more than a hundred samples, GS 4 lignins could have a roughly estimated composition of 70–45% of S, 50–25% of G, and 5–0% of H (Faix 1991). These results agreed with Culebras et al. (2018a), who studied bio-based polymers based on lignin. Their results described variations of intensity for those characteristic lignin bands depending on lignin content of blended materials. Dávila et al. (2019) also reported these lignin-related bands while studying lignin production through hydrothermal pretreatment followed by simultaneous saccharification and fermentation (Ståhl et al. 2018). Likewise, Trubetskaya et al. (2020) reported similar spectra while characterizing organosolv lignins from wood and other herbaceous feedstocks.

Nuclear magnetic resonance spectroscopy (NMR) was performed to validate FTIR results (Fig. 3b, c). The solubility of the samples is reported in Table S5. While samples LG4 and LG1.5 were fully soluble in DMSO, EHL was only partially soluble, and HTBW and MBW were insoluble. This trend was reversed when using chloroform as the solvent. LG4 was the sample showing the most intense lignin related signals with the presence of  $\beta$ -O-4 and  $\beta$ - $\beta$  bonds. The presence of methoxy groups is also evident, which implies the presence of S units. The lack of intensity for NMR signals is attributed to high carbohydrate content in those samples which interferes with the solubilization step.

## Thermogravimetric behaviour of LRSs

The first thermal zone below 180 °C may be associated with residual moisture content on the samples and thermal evolution of low molecular weight species (Ståhl et al. 2018). The second degradation zone between 180 and 400 °C is related to carbohydrates and extractives (Li and McDonald 2014; Rowlandson et al. 2020; Watkins et al. 2015). The second degradation zone is further related to the breakout of labile  $\beta$ -O-4 linkages (Guo et al. 2015). The third degradation zone between 400 and 500 °C is related to carbonyl groups, methanol and methane evolution (Culebras et al. 2018b; Trubetskaya et al. 2020). Finally, the degradation zone above 500 °C is related to volatile components, including phenolics, alcohols, aldehyde acids etc. (Rowlandson et al. 2020; Wądrzyk et al. 2021). Table S7 shows the maximum weight loss temperature ( $T_{max}$ ), the  $T_g$  and the carbon yield of the LRSs at the end of the analysis. The first derivative curves (dTG) and weight loss percentage (TGA curves) are shown in Fig. 4a, c. In Fig. 4b, the woodish samples (MBW and HTBW) did not present a clear inflection point attributed to their lack of innate thermoplasticity, whereas all the LRSs showed glass transition behaviour. The LG1.5 presented a  $T_g$  (120 °C), with EHL (150 °C), and the LG4 with the lowest (96 °C). These results indicate that materials are suitable for blending with other thermoplastic polymers to produce polymer blends with optimized thermal performance.

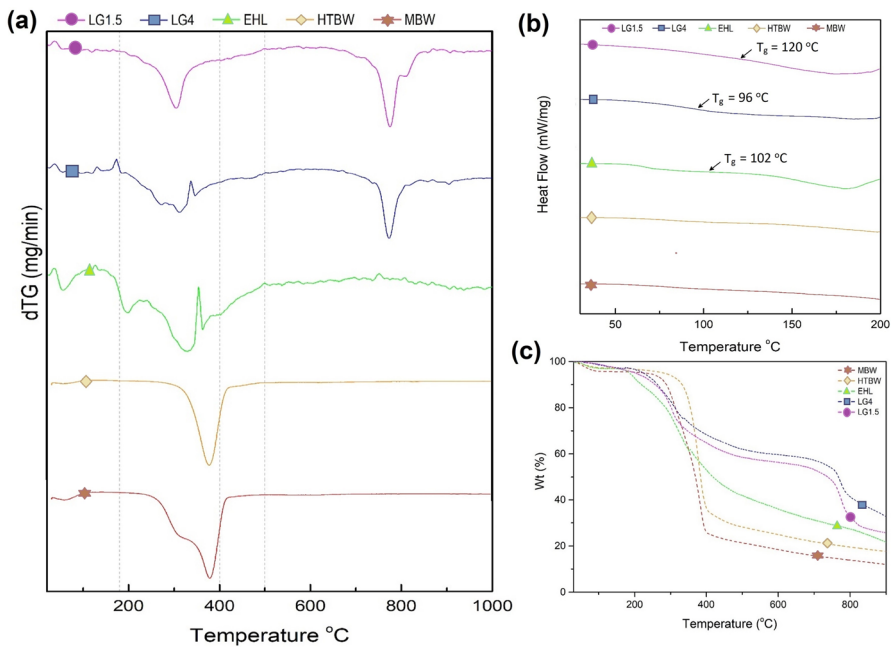


**Fig. 4** a TGA—first derivative curves of lignin produced by enzymatic hydrolysis or kraft process; **b** DSC—temperature heat flow curves of lignin produced by enzymatic hydrolysis or kraft process; **c** TGA—weight loss of lignin produced by enzymatic hydrolysis or kraft process

The  $T_g$  values recorded here are in line with other studies (Li and McDonald 2014; Rowlandson et al. 2020).

Figure 4c shows that, samples lost 3% of their mass during the first degradation zone, attributed to their minimum moisture content. The MBW presented a shoulder at 309 °C followed by the primary degradation step at 377 °C attributed to hemicellulose and cellulose, respectively. In contrast, the HTBW show degradation only at 379 °C; this confirms the pretreatment effectiveness to remove carbohydrates derived from hemicellulose. Although all the LRSs show significant weight loss in the second degradation zone, each sample exhibited distinct profiles due to differences in carbohydrate content.

Both kraft lignins (LG and LG1.5) exhibit a slight slope above 350 °C, related to small but continuous degradation attributed to labile bonds, followed by a slower thermal degradation until below 800 °C where sharp increase in rate occurs (Rinaldi et al. 2016). While the EHL was approximately 60% degraded at 500 °C, which indicates the homogeneity of its polymeric chain in comparison to kraft lignins. The kraft lignins are more thermally stable and have higher carbon yields. This is ascribed to the introduction of strong C–C bonds during the kraft process (Rios et al. 2006; Watkins et al. 2015). On the other hand, the EHL, HTBW, and MBW exhibit lower carbon yields due to their structure with weaker chemical bonds such as glycosidic C–O–C,  $\beta$ -O-4 linkages, methoxyl and methyl groups prevalent (Rios et al. 2006; Ståhl et al. 2018).

### Surface area and pore size analysis of LRSs

During hydrothermal pretreatment, the physical structure of the pretreated samples changed, affecting their available surface area and pore size distribution (PoSD). Thus, it was decided to conduct gas sorption analysis on the samples to evaluate these properties. Furthermore, lignin-rich substrates' surface and pore characterization provide valuable information regarding potential engineering applications.

The surface area of the MBW increased after going through hydrothermal pretreatment from an initial 1.2–3.7 m<sup>2</sup>/g representing an increment of 197% as shown in Table 1. On the other hand, all the EHLs show a similar surface area with values in the range of 5.1–5.6 m<sup>2</sup>/g, indicating that the enzymatic treatment did not significantly impact the sample's physical structure. However, before enzymatic hydrolysis, the HTBW (200 °C) had a more accessible surface than the HTBW (170 °C), but during enzymatic hydrolysis of the HTBW (200 °C), less cellulose was digested (Table S1). This result suggested that the lower performance of the enzymes for digesting cellulose out of the HTBW (200 °C) was not related to a physical hindrance. Therefore, this provides further evidence that cellulases may be getting absorbed into the lignin as described earlier.

On the other hand, the average pore size distribution of the MBW also increased after hydrothermal pretreatment from an initial 11 nm to values circa 18 nm for the HTBWs and 21 nm for the EHLs. Notably, the HTBWs pores were mainly located around a pore width of 1, 12 and 50 nm, corresponding to the severity of the treatment (170 °C, 190 °C and 200 °C). Thus, results agree with the surface area values,

**Table 1** Surface and pore size distribution of produced lignin-rich substrates

Description	BET (m <sup>2</sup> /g)	Total pore volume (cc/g)	Average PoSD (nm)	Mainly located pores (QSDFT)
MBW	1.2	0.00	11	1
HTBW (170°)	2.3	0.01	15	1
HTBW (190°)	2.9	0.01	21	12
HTBW (200°)	3.7	0.02	19	50
EHL (170°)	5.6	0.03	18	50
EHL (190°)	5.1	0.03	23	50
EHL (200°)	5.2	0.03	23	50
LG4 (140°)	0.2	0.00	16	28
LG4 (170°)	0.5	0.00	10	5
LG4 (190°)	0.5	0.00	6	5

*PoSD* pore size distribution, *QSDFT* quenched solid density functional theory

confirming the hydrothermal pretreatment impact on the physical structure of the samples (Lowell et al. 2012). Isotherm and PoSD plots are shown in Figure S2, S3, and S4.

The isotherm of the HTBWs and EHLs corresponded to a type II Isotherm, associated with macroporous samples (Thommes et al. 2015). The isotherm remains close to  $P/P_0 \sim 1$  indicating an abundance of macropores (Lowell et al. 2012). Figure S3 shows the formation of new pore regions after the accessible cellulose is digested. Figure S4 shows peaks representing the pores' central location and their cumulative surface area, which increased, as expected, after enzymatic hydrolysis. For EHLs new pores appear, and these new pores increased the surface area of the enzymatically treated sample, as shown in Figure S4 with a broad band starting at 25 nm, corresponding to the first derivative. The cumulative surface area spikes after the 25 nm region, confirming the new pores' central location. For kraft lignin unexpectedly low values are recorded, with values pointing towards the micro-pore region.

### Morphological analysis of LRSs

The untreated, hydrothermally pretreated, and enzymatically treated birch wood are illustrated in Fig. 5a–c, respectively, showing the clear impact of pretreatment on the sample surface. The main characteristics noticed is the fibrous morphology with the presence of cracks, nodules, and sharp-pointed edges appearing from sample fissures. Figure 5c shows the morphology of the sample when cellulose has been digested by enzymatic hydrolysis. Evenly defined channels with jagged edges are observed. The images confirm the woodish appearance of the enzymatic residue, as shown in Table S2, still has recalcitrant cellulose that has not been digested despite increasing the enzyme dosage. Further refinement needs to be done on the EHLs to upgrade the lignin present in the enzymatic residue. Figure 5d, e reveals the morphological macro-disposition of the kraft lignins. Compared to the previous images,

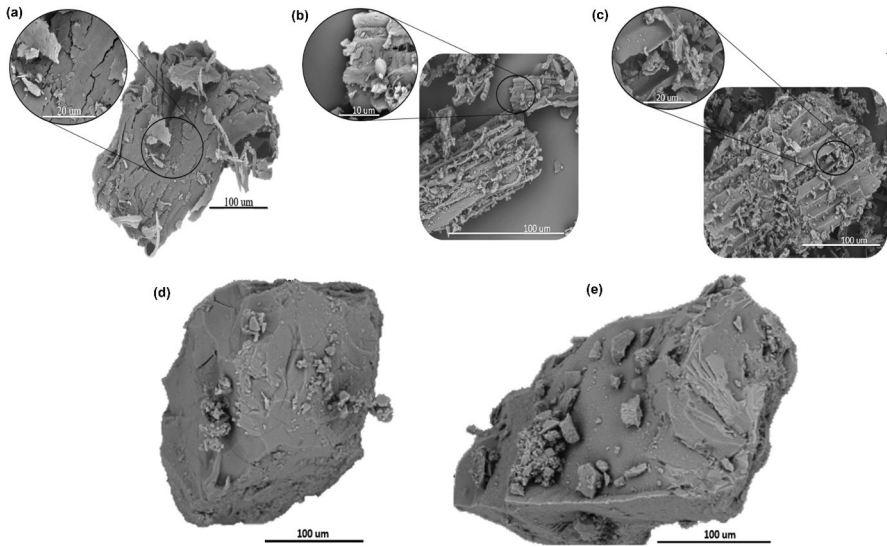


**Fig. 5** Scanning electron microscopy images of **a** milled birch wood (MBW), **b** pretreated birch wood (HTBW), and **c** enzymatic hydrolysis lignin (EHL); and kraft lignin precipitated as pH 4 and 1.5 **d** LG 4 and **e** LG1.5

the samples look like granules without a woodish or fibrous appearance. Taken over all these images support the BET surface area results.

## Conclusion

Lignin fractionation and recovery from pulp and bioethanol industry waste offer a promising avenue to convert ecological challenges into sustainable biomaterial solutions. Customization is paramount due to the distinct composition and characteristics of raw technical lignins. Notably, higher hydrothermal pretreatment temperatures, particularly at 190 °C, substantially enhance cellulose surface area, yielding enzymatic hydrolysis lignins (EHLs) with an excellent 66.4% lignin content, while kraft lignins consistently demonstrate high lignin content across various conditions. Kraft lignins exhibit a carbon-rich composition (63.0%) with lower hydrogen content (3.8%), indicating greater resistance to hydrogen degradation under harsh processing conditions compared to EHLs. However, sulphur contamination in kraft lignins due to sulphuric acid precipitation is notable, albeit necessary for yield. FTIR analysis validates the presence of aromatic skeletons and methoxyl groups in all lignin-rich substrates, emphasizing sample purity's role in determining chemical structure. Additionally, differential scanning calorimetry highlights that EHLs possess lower glass transition temperatures, making them suitable for thermoplastic blending and valorization, while kraft lignin exhibits resilience to thermal degradation at higher temperatures, making them potentially valuable for applications such as carbon fibres and activated carbon production. Surface area values are relatively

low for both lignins. Overall, this research underscores the potential of lignin fractionation to contribute to a sustainable and circular economy by repurposing industrial waste into valuable biomaterials.

**Supplementary Information** The online version contains supplementary material available at <https://doi.org/10.1007/s00226-024-01531-8>.

**Acknowledgements** Celignis Ltd for financial and analytical support of ER.

**Author contributions** ER and MNC wrote the main manuscript text and MM prepared Figs. 1, 2, 3, 4, and 5 and supplementary information. All authors reviewed the manuscript.

**Funding** Open Access funding provided by the IReL Consortium.

## Declarations

**Conflict of interest** The authors declare no competing interests.

**Open Access** This article is licensed under a Creative Commons Attribution 4.0 International License, which permits use, sharing, adaptation, distribution and reproduction in any medium or format, as long as you give appropriate credit to the original author(s) and the source, provide a link to the Creative Commons licence, and indicate if changes were made. The images or other third party material in this article are included in the article's Creative Commons licence, unless indicated otherwise in a credit line to the material. If material is not included in the article's Creative Commons licence and your intended use is not permitted by statutory regulation or exceeds the permitted use, you will need to obtain permission directly from the copyright holder. To view a copy of this licence, visit <http://creativecommons.org/licenses/by/4.0/>.

## References

- Albadarin AB, Collins MN, Naushad M, Shirazian S, Walker G, Mangwandi C (2017) Activated lignin-chitosan extruded blends for efficient adsorption of methylene blue. *Chem Eng J* 307:264–272. <https://doi.org/10.1016/j.cej.2016.08.089>
- Araújo LCP, Yamaji FM, Lima VH, Botaro VR (2020) Kraft lignin fractionation by organic solvents: Correlation between molar mass and higher heating value. *Bioresour Technol* 314:123757. <https://doi.org/10.1016/j.biortech.2020.123757>
- Beaucamp A, Wang Y, Culebras M, Collins MN (2019) Carbon fibres from renewable resources: the role of the lignin molecular structure in its blendability with biobased poly(ethylene terephthalate). *Green Chem* 21(18):5063–5072. <https://doi.org/10.1039/C9GC02041A>
- Beaucamp A, Muddasar M, Amiin IS, Moraes Leite M, Culebras M, Latha K, Gutiérrez MC, Rodríguez-Padron D, del Monte F, Kennedy T, Ryan KM, Luque R, Titirici M-M, Collins MN (2022a) Lignin for energy applications—state of the art, life cycle, technoeconomic analysis and future trends. *Green Chem* 24(21):8193–8226. <https://doi.org/10.1039/D2GC02724K>
- Beaucamp A, Muddasar M, Crawford T, Collins MN, Culebras M (2022b) Sustainable lignin precursors for tailored porous carbon-based supercapacitor electrodes. *Int J Biol Macromol* 221:1142–1149. <https://doi.org/10.1016/j.ijbiomac.2022.09.097>
- Beaucamp A, Muddasar M, Culebras M, Collins MN (2024) Sustainable lignin-based carbon fibre reinforced polyamide composites: production, characterisation and life cycle analysis. *Compos Commun* 45:101782. <https://doi.org/10.1016/j.coco.2023.101782>
- Borrega M, Nieminen K, Sixta H (2011) Effects of hot water extraction in a batch reactor on the delignification of birch wood. *BioResources* 6:1890–1903. <https://doi.org/10.15376/biores.6.2.1890-1903>
- Chang HM, Cowling EB, Brown W (1975) Comparative studies on cellulolytic enzyme lignin and milled wood lignin of sweetgum and spruce. *Holzforschung* 29:153–159

- Chen L, Wang X, Yang H, Lu Q, Li D, Yang Q, Chen H (2015) Study on pyrolysis behaviors of non-woody lignins with TG-FTIR and Py-GC/MS. *J Anal Appl Pyrol* 113:499–507. <https://doi.org/10.1016/j.jaap.2015.03.018>
- Collins MN, Nechifor M, Tanasă F, Zănoagă M, McLoughlin A, Strózyk MA, Culebras M, Teacă C-A (2019) Valorization of lignin in polymer and composite systems for advanced engineering applications—a review. *Int J Biol Macromol* 131:828–849. <https://doi.org/10.1016/j.ijbiomac.2019.03.069>
- Culebras M, Beaucamp A, Wang Y, Clauss MM, Frank E, Collins MN (2018a) Biobased structurally compatible polymer blends based on lignin and thermoplastic elastomer polyurethane as carbon fiber precursors. *ACS Sustain Chem Eng* 6(7):8816–8825. <https://doi.org/10.1021/acssuschemeng.8b01170>
- Culebras M, Sanchis MJ, Beaucamp A, Carsí M, Kandola BK, Horrocks AR, Panzetti G, Birkinshaw C, Collins MN (2018b) Understanding the thermal and dielectric response of organosolv and modified kraft lignin as a carbon fibre precursor. *Green Chem* 20(19):4461–4472. <https://doi.org/10.1039/C8GC01577E>
- Dalton N, Lynch RP, Collins MN, Culebras M (2019) Thermoelectric properties of electrospun carbon nanofibres derived from lignin. *Int J Biol Macromol* 121:472–479. <https://doi.org/10.1016/j.ijbiomac.2018.10.051>
- Dávila I, Gullón B, Labidi J, Gullón P (2019) Multiproduct biorefinery from vine shoots: bio-ethanol and lignin production. *Renew Energy* 142:612–623. <https://doi.org/10.1016/j.renene.2019.04.131>
- Ewanick SM, Bura R, Saddler JN (2007) Acid-catalyzed steam pretreatment of lodgepole pine and subsequent enzymatic hydrolysis and fermentation to ethanol. *Biotechnol Bioeng* 98(4):737–746. <https://doi.org/10.1002/bit.21436>
- Faix O (1991) Classification of lignins from different botanical origins by FT-IR spectroscopy. *Holzforchung* 45(s1):21–28. <https://doi.org/10.1515/hfsg.1991.45.s1.21>
- Galbe M, Wallberg O (2019) Pretreatment for biorefineries: a review of common methods for efficient utilisation of lignocellulosic materials. *Biotechnol Biofuels* 12:1–26
- Guo Y, Zhou J, Wen J, Sun G, Sun Y (2015) Structural transformations of triploid of *Populus tomentosa* Carr. lignin during auto-catalyzed ethanol organosolv pretreatment. *Ind Crops Prod* 76:522–529. <https://doi.org/10.1016/j.indcrop.2015.06.020>
- Hayes DJM (2013) Chapter 2—Biomass composition and its relevance to biorefining. In: Triantafyllidis KS, Lappas AA, Stöcker M (eds) *The role of catalysis for the sustainable production of bio-fuels and bio-chemicals*. Elsevier, Amsterdam, pp 27–65. <https://doi.org/10.1016/B978-0-444-56330-9.00002-4>
- Helander M, Theliander H, Lawoko M, Henriksson G, Zhang L, Lindström M (2013) Fractionation of technical lignin: molecular mass and pH effects. *BioResources*. <https://doi.org/10.15376/biores.8.2.2270-2282>
- Hu Z, Yeh T-F, Chang H-M, Matsumoto Y, Kadla JF (2006) Elucidation of the structure of cellulolytic enzyme lignin. *Holzforchung* 60(4):389–397. <https://doi.org/10.1515/HF.2006.061>
- Hussin MH (2014) Extraction, modification and characterization of lignin from oil palm fronds as corrosion inhibitors for mild steel in acidic solution. Université de Lorraine, Thesis
- Jędrzejczak P, Collins MN, Jesionowski T, Klapiszewski Ł (2021) The role of lignin and lignin-based materials in sustainable construction—a comprehensive review. *Int J Biol Macromol* 187:624–650. <https://doi.org/10.1016/j.ijbiomac.2021.07.125>
- Li H, McDonald AG (2014) Fractionation and characterization of industrial lignins. *Ind Crops Prod* 62:67–76. <https://doi.org/10.1016/j.indcrop.2014.08.013>
- Lowell S, Shields JE, Thomas MA, Thommes M (2012) Characterization of porous solids and powders: surface area, pore size and density, Particle Technology Series (POTS, volume 16). Springer, Berlin
- Lu Y-C, Lu Y, Fan X (2020) Structure and characteristics of lignin. In: Sharma S, Kumar A (eds) *Lignin: biosynthesis and transformation for industrial applications*. Springer, Berlin, pp 17–75. [https://doi.org/10.1007/978-3-030-40663-9\\_2](https://doi.org/10.1007/978-3-030-40663-9_2)
- Mooney CA, Mansfield SD, Touhy MG, Saddler JN (1998) The effect of initial pore volume and lignin content on the enzymatic hydrolysis of softwoods. *Bioresour Technol* 64(2):113–119. [https://doi.org/10.1016/S0960-8524\(97\)00181-8](https://doi.org/10.1016/S0960-8524(97)00181-8)
- Muddasar M, Liaquat R, Aslam A, Ur Rahman MZ, Abdullah A, Khoja AH, Latif K, Bahadar A (2022) Performance efficiency comparison of microbial electrolysis cells for sustainable production of bio-hydrogen—a comprehensive review. *Int J Energy Res* 46(5):5625–5645. <https://doi.org/10.1002/er.7606>

- Muddasar M, Liaquat R, Rahman MZU, Khoja AH, Aslam A, Basit A (2023a) Coaxial microbial electrolysis cell for cost-effective bioenergy production and wastewater treatment of potato industry effluent. *J Chem Technol Biotechnol*. <https://doi.org/10.1002/jctb.7433>
- Muddasar M, Nasiri MA, Cantarero A, Gómez C, Culebras M, Collins MN (2023b) Lignin-derived ionic conducting membranes for low-grade thermal energy harvesting. *Adv Funct Mater* 2306427. <https://doi.org/10.1002/adfm.202306427>
- Muddasar M, Mushtaq M, Beaucamp A, Kennedy T, Culebras M, Collins MN (2024) Synthesis of sustainable lignin precursors for hierarchical porous carbons and their efficient performance in energy storage applications. *ACS Sustain Chem Eng*. <https://doi.org/10.1021/acssuschemeng.3c07202>
- Nakagame S, Chandra RP, Saddler JN (2010) The effect of isolated lignins, obtained from a range of pretreated lignocellulosic substrates, on enzymatic hydrolysis. *Biotechnol Bioeng* 105(5):871–879. <https://doi.org/10.1002/bit.22626>
- Nakagame S, Chandra RP, Kadla JF, Saddler JN (2011) The isolation, characterization and effect of lignin isolated from steam pretreated Douglas-fir on the enzymatic hydrolysis of cellulose. *Biore-sour Technol* 102(6):4507–4517. <https://doi.org/10.1016/j.biortech.2010.12.082>
- Patt R, Kordsachia O, Süttinger R, Ohtani Y, Hoesch JF, Ehrler P, Eichinger R, Holik H, Hamm U, Rohmann ME, Mummehoff P, Petermann E, Miller RF, Frank D, Wilken R, Baumgarten HL, Rentrop G-H (2000) Paper and pulp. In: Ullmann's encyclopedia of industrial chemistry. [https://doi.org/10.1002/14356007.a18\\_545](https://doi.org/10.1002/14356007.a18_545)
- Rinaldi R, Jastrzebski R, Clough MT, Ralph J, Kennema M, Bruijninx PCA, Weckhuysen BM (2016) Paving the way for lignin valorisation: recent advances in bioengineering, biorefining and catalysis. *Angew Chem Int Ed* 55(29):8164–8215. <https://doi.org/10.1002/anie.201510351>
- Rios RVRA, Martínez-Escandell M, Molina-Sabio M, Rodríguez-Reinoso F (2006) Carbon foam prepared by pyrolysis of olive stones under steam. *Carbon* 44(8):1448–1454. <https://doi.org/10.1016/j.carbon.2005.11.028>
- Rowlandson JL, Woodman TJ, Tennison SR, Edler KJ, Ting VP (2020) Influence of aromatic structure on the thermal behaviour of lignin. *Waste Biomass Valoriz* 11(6):2863–2876. <https://doi.org/10.1007/s12649-018-0537-x>
- Rubio MC, Beaucamp A, Stróżyk MA, Collins MN (2022) Lignin-based carbon fibers for high performance green composites. In: Baskar C, Ramakrishna S, Daniela La Rosa A (eds) *Encyclopedia of green materials*. Springer Nature, Singapore, pp 1–8. <https://doi.org/10.1007/978-981-16-4921-9%5F155-1>
- Sharma S, Sharma A, Mulla SI, Pant D, Sharma T, Kumar A (2020) Lignin as potent industrial biopolymer: an introduction. In: Sharma S, Kumar A (eds) *Lignin: biosynthesis and transformation for industrial applications*. Springer, Berlin, pp 1–15. [https://doi.org/10.1007/978-3-030-40663-9\\_1](https://doi.org/10.1007/978-3-030-40663-9_1)
- Sluiter A, Hames B, Ruiz R, Scarlata C, Sluiter J, Templeton D, Crocker D (2008) Determination of structural carbohydrates and lignin in biomass. Laboratory Analytical Procedure (LAP), National Renewable Energy Laboratory
- Ståhl M, Nieminen K, Sixta H (2018) Hydrothermolysis of pine wood. *Biomass Bioenergy* 109:100–113. <https://doi.org/10.1016/j.biombioe.2017.12.006>
- Thommes M, Kaneko K, Neimark AV, Olivier JP, Rodríguez-Reinoso F, Rouquerol J, Sing KSW (2015) Physisorption of gases, with special reference to the evaluation of surface area and pore size distribution (IUPAC Technical Report). *Pure Appl Chem* 87(9–10):1051–1069. <https://doi.org/10.1515/pac-2014-1117>
- Trubetskaya A, Lange H, Wittgens B, Brunsvik A, Crestini C, Rova U, Christakopoulos P, Leahy JJ, Matsakas L (2020) Structural and thermal characterization of novel organosolv lignins from wood and herbaceous sources. *Processes* 8(7):860
- Wądrzyk M, Janus R, Lewandowski M, Magdziarz A (2021) On mechanism of lignin decomposition—investigation using microscale techniques: Py-GC-MS, Py-FT-IR and TGA. *Renew Energy* 177:942–952. <https://doi.org/10.1016/j.renene.2021.06.006>
- Watkins D, Nuruddin M, Hosur M, Tcherbi-Narteh A, Jeelani S (2015) Extraction and characterization of lignin from different biomass resources. *J Mater Res Technol* 4(1):26–32. <https://doi.org/10.1016/j.jmrt.2014.10.009>
- Zhao J, Xiuwen W, Hu J, Liu Q, Shen D, Xiao R (2014) Thermal degradation of softwood lignin and hardwood lignin by TG-FTIR and Py-GC/MS. *Polym Degrad Stab* 108:133–138. <https://doi.org/10.1016/j.polymdegradstab.2014.06.006>

Zhu W, Theliander H (2015) Precipitation of lignin from softwood black liquor: an investigation of the equilibrium and molecular properties of lignin. *BioResources*. <https://doi.org/10.15376/biores.10.1.1696-1715>

**Publisher's Note** Springer Nature remains neutral with regard to jurisdictional claims in published maps and institutional affiliations.